Microchimica Acta (2021) 188: 394
https://doi.org/10.1007/s00604-021-05041-3

SHORT COMMUNICATION

Lab-made 3D-printed accessories for spectroscopy and spectroelectrochemistry: a proof of concept to investigate dynamic interfacial and surface phenomena

Joadir Humberto da Silva Junior[1] · Jailson Vieira de Melo[1] · Pollyana Souza Castro[1]

Received: 27 July 2021 / Accepted: 26 September 2021 / Published online: 27 October 2021

Abstract

3D printing is presented as an auspicious additive manufacturing technique for diverse interesting applications coupling electrochemistry and spectroscopy techniques, proposing as utilities: a general-purpose module for specular spectroscopy and spectroelectrochemical (SEC) cells for in situ UV-VIS and Raman measures capable of acting in flux or a stationary regime. As a proof of concept, UV-VIS absorption and middle-infrared spectra of an azo dye thin film were collected with the specular module showing characteristic bands according to the literature data. SEC investigations related to the Prussian Blue (PB) film growth on the platinum electrode surface were also investigated. By applying appropriate potentials, the PB film growth was accompanied by a proportional increase in the absorption signal at 700 nm in the UV-VIS region. This signal was related to the intervalence charge transfer from the Fe(II)-C to Fe(III)-N. Moreover, the Raman SEC experiment presented scattering intensity at 2092 and 2156 cm^{-1}, related to the (CN) mode associated with the Fe(II) and Fe(III) cations, which was observed during the thin film growth. In addition, the conversion to the Berlin Green (BG) and Prussian White (PB) forms was monitored while applying the suitable potential and in situ spectroscopic observations of structural changes during the redox processes were also detected as described in the literature. Thus, it is possible to state that the accessories successfully validated in situ spectroelectrochemical dynamic investigations unlocking many other applications in this research field.

Keywords 3D printing · Additive manufacturing · Lab-made accessories · Spectroscopy · Spectroelectrochemistry · Thin film growth · Dynamic surface phenomena

Introduction

Electrochemical processes take place of reactions caused or accompanied by the passage of electrical current for different purposes. In general, this process involves electron transfer between a solid conductor (an electrode) and a substance dispersed in an electrolytic medium. In this way, the electrochemical reaction can be induced in different ways: by maintaining an electrical potential for a certain time and adjusting it so that a certain current density is maintained throughout the process [1]. In many situations, it is extremely relevant to elucidate unknown electrogenerated intermediates or products to obtain information concerning the reaction mechanism adjacent to/or on the surface of a non-transparent electrode. By combining electrochemical and spectroscopic techniques such as UV-VIS and infrared absorption spectroscopy, as well as Raman microspectroscopy, real-time powerful data can be obtained to understand the reaction steps avoiding misinterpretation [2, 3]. This research area can conveniently perform ex situ investigations by using accessories for specular reflectance although in situ observations demand a very particular spectroelectrochemical (SEC) cell [4, 5].

Accessories for these purposes are easily found on the market, but often difficult to purchase due to the high cost, the exclusivity of parts from the manufacturers, and consequent low versatility. Thus, an alternative found by many research groups has been the homemade construction of the

This article is part of the Topical Collection on *3D printing manufacturing technologies for the advancement of analytical sciences*

✉ Pollyana Souza Castro
pollyana.castro@ufrn.br

[1] Federal University of Rio Grande do Norte, Institute of Chemistry, Lagoa Nova - CEP 59.072-970, Natal, RN, Brazil

own accessories [6, 8], including recent projects using 3D printing technology [6–14]. This additive manufacturing technique can be considered fast, low cost, and sustainable, with a great capacity for customization of complex structures, in particular, internal structures [9–11]. Furthermore, many models can be easily downloaded on the Internet and modified and reproduced according to the user's needs around the world [15–20].

This work used 3D printing technology to develop a series of accessories aiming to integrate ex situ or in situ electrochemical and spectroscopic techniques to investigate dynamic interfacial and surface phenomena, such as an accessory for specular reflectance, an SEC for UV-VIS investigation, and an SEC for Raman microspectroscopy analysis capable of acting in flux or in a stationary regime. The cells were designed to be used with the available equipment with minimum complexity for the interface, in a compatible way with common commercial electrodes, and especially as a simple, low-cost, low-time production, and sustainable open-lab alternative, allowing, with few design modifications, the capacity to be used in different instruments and conditions.

Experimental section

All chemicals and suppliers employed in this work are listed in the Supporting Information Section S.1.1.

Apparatus

The electrochemical processes were controlled by a BASi Epsilon Potentiostat/Galvanostat, using a system made of three electrodes: a homemade platinum disc electrode (⌀6 mm) as working electrode (see in the Supporting Information Section S.2 the Design and characterization) and an Ag/AgCl (3M KCl) and a platinum wire as reference and auxiliary electrodes, respectively. All accessories were designed to replace the original spectrometers sample holders. The equipment used in the investigations were Shimadzu UV-1800 for UV-VIS acquisition, Perkin Elmer Frontier for middle-infrared region (mid-IR), and a Horiba LabRAM HR Evolution for Raman microspectrometry.

Accessories design

All printable parts were designed using a free and online 3D app Tinkercad™ (https://www.tinkercad.com). The models were sliced using the Ultimaker Cura™ app (https:// https://ultimaker.com/) to create G-Code instruction archives used by the homemade 3D printer (based on RepRap Ormerod). The specular reflectance module and SEC cells were made using black color ⌀1.75 mm PETg filament (3DFila, Brazil). The material was chosen based on its good chemical and high impact resistance, great durability and ease of printing—even without a heated bed—to prevent spurious contribution by undesirable scattering radiation. The 3D printing settings are described in the Supporting Information Section S.1.2. Figure 1 shows all accessories fabricated in this work.

The specular reflectance module (Fig.1a) was designed to adapt two plane mirrors in angle. The first one deflects radiation to the sample surface—which must be placed face-down—and a second one deflects the component of radiation specularly reflected by the substrate that supports the sample back to the original direction. A similar arrangement was used to construct in situ UV-VIS SEC (Fig. 2b). In this case, the sample surface of the working electrode was vertically disposed and enclosed into a cell. A quartz window (⌀20 x 1 mm) was allowed to interact between the radiation and electrode surface. Finally, the in situ Raman SEC (Fig. 1c) was designed to obtain the working electrode surface facing upwards, capable of receiving an array of three or more electrodes and adapters to perform dynamic flux measurements. The same quartz window of UV-Vis SEC (⌀20 x 1 mm) can be used if the electrolytic medium offers a corrosion risk to the microscope objective or allows flow within the cell. More details about the accessory fabrication are described in the Supporting Information Section S.3.

Spectroelectrochemistry analysis

The accessories performance was evaluated using some materials and processes with predictable spectroscopic behavior and extensive discussions in the literature. In the specular reflectance module case, a thin film of Allura Red AC was deposited on the surface of an aluminum disc. The Supporting Information Section S.4 shows the colorant structural formula and the sample preparation procedure. The spectrums were recorded for UV-VIS and mid-IR regions. As a proof of concept for the SEC cells, an electrodeposition of Prussian Blue (PB) film in the lab-made Pt working electrode using 0.1 mol L^{-1} KCl solution as supporting electrolyte was performed. By the potentiostat mediation, a potential of + 0.3 V *vs.* Ag/AgCl (3M KCl) was applied during 200 s promoting the reaction between potassium ferricyanide and ferric chloride. Continuous absorbance measurements were taken at 700 nm for UV-VIS SEC or a spectrum in the region between 1600 and 2600 cm^{-1} (using 633 nm laser) every 20 s with the Raman SEC cell. The conversion of this film to the Berlin Green (BG) and Prussian White (PW) forms was carried out by the application of the appropriate potential −0.3 and 1.1 V for PW and BG, respectively.

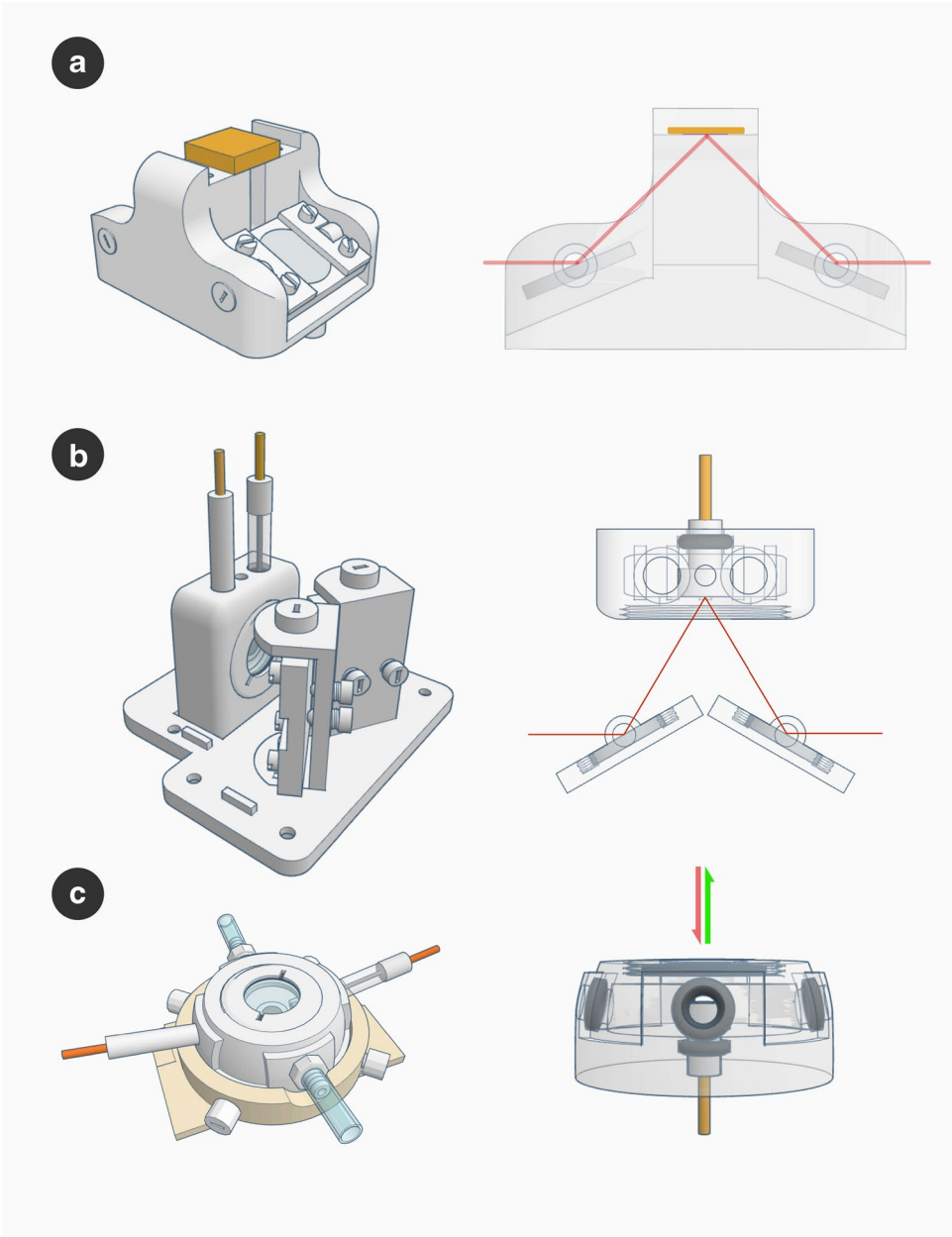

Fig. 1. Lab-made 3D-printed accessories projects: (**a**) Specular reflectance module for ex-situ UV-VIS-NIR and FTIR measurements. (**b**) Spectro-electrochemical cell for *in situ* UV-VIS measurements. (**c**) Spectroelectrochemical cell for in situ Raman microspectrometry

Results and discussions

All printed pieces had dimensions that were identical to the projects they were based on, which ensured a good and reliable connection between all pluggable/threadable pieces. The accessories preserved their shape for a long time and showed no signs of moisture absorption or degradation that would hamper the integrity or purpose that they were developed. The time required for the prints was approximately 42 h (18 h for both the reflectance module and UV-VIS SEC and 6 h for Raman SEC), by an estimated cost of around 15 $ per unit. High-quality, leak-free devices Fig. 2 shows the 3D-printed reflectance module, UV-VIS SEC, and Raman SEC cells.

Allura Red AC is a synthetic azo dye whose chromophore properties are based on the presence of an azo group (R-N=N-R'), which is connected to the auxochrome hydroxy and methoxy groups through aromatic π-system rings. The colorant presented a characteristic absorption band at 500 nm on the visible region (Fig. 3a). The spectra for the mid-IR region show the characteristics bands at 3445 (hydroxy), 1500 (azo), and at 1040 and 1060 cm^{-1} (sulfonate groups). All the results were in agreement with the database and current literature [21, 22] showing that the accessories are very suitable for this investigation approach.

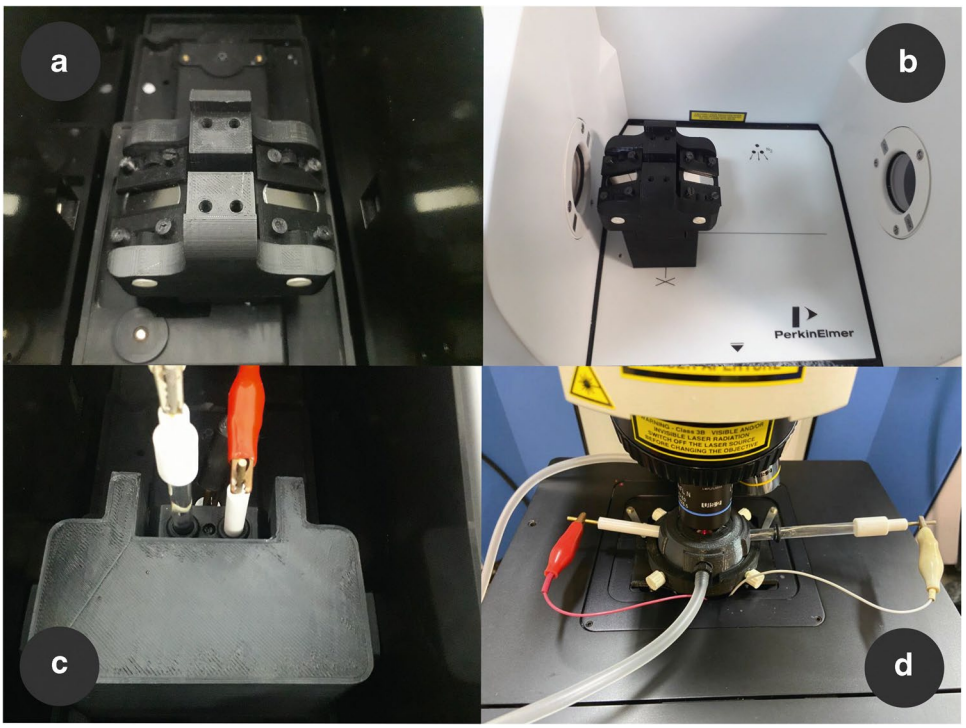

Fig. 2 Lab-made 3D-printed accessories installed in the commercial equipment: Specular reflectance module for *ex situ* UV-VIS-NIR and FTIR measurements coupled in a (**a**) Shimadzu UV-1800 UV-VIS spectrophotometer and (**b**) Perkin Elmer Frontier FTIR spectrometer. (**c**) Spectroelectrochemical cell for in situ UV-VIS measurements coupled in a Shimadzu UV-1800 UV-VIS spectrophotometer. (**d**) Spectroelectrochemical cell for in situ Raman microspectrometry installed in a Horiba LabRAM HR Evolution Raman microspectrometer

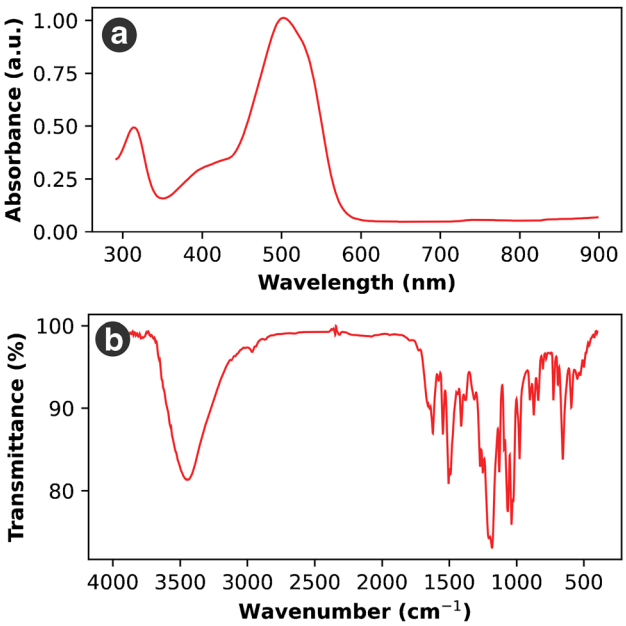

Fig. 3 (**a**) UV-VIS and (**b**) mid-IR spectra for Allura Red AC film deposited on the surface of an aluminum mirror obtained with the lab-made 3D-printed accessory for ex situ specular reflectance measurements

The performance of the UV-VIS and Raman SECs was evaluated by monitoring the Prussian Blue (PB) growth film process [23]. The SECs were mounted in the respective spectrometers using a three-electrode electrochemical system. The reaction was promoted from the mixture of 4.0, 1.0, and 1.0 mL of 0.1 mol L^{-1} potassium chloride; 10 mmol L^{-1} potassium ferricyanide; and 10 mmol L^{-1} ferric chloride solutions, respectively. After the addition of the last component, a potential equal to + 0.3 V was applied and maintained for 200 s, while continuous absorbance measurements were taken at 700 nm for UV-VIS SEC—maximum absorption for the PB or a spectrum in the region between 1600 and 2600 cm^{-1} (using 633 nm laser) every 20 s in the Raman case [24]. The film electrosynthesis process follows the reaction between hexacyanoferrate (II) and ferric chloride (Eqs. 1 and 2).

$$\left[Fe^{(III)}(CN)_6\right]^{3-} + e^- \rightleftarrows \left[Fe^{(II)}(CN)_6\right]^{4} \quad (1)$$

$$4Fe^{3+} + 3\left[Fe^{(II)}(CN)_6\right]^{4-} \longrightarrow Fe_4{}^{(III)}\left[Fe^{(II)}(CN)_6\right]_3 \quad (2)$$

In the first case, the absorption index at 700 nm—maximum absorption for the PB—during the process was monitored. Fig. 4a shows the increase in the absorption while applying the suitable potential with PB film growing at the electrode surface. In the in situ Raman monitoring (Fig. 4b), the signal at 2200 cm^{-1} increased due to the presence of (CN) bands between 2000 and 2200 cm^{-1}.

In addition, the electrochemical conversion of PB film into the Prussian White (PW) and Berlin Green (BG) redox states was also real-time accompanied. For conversion to PW and BG forms, the electrolyte medium was changed to

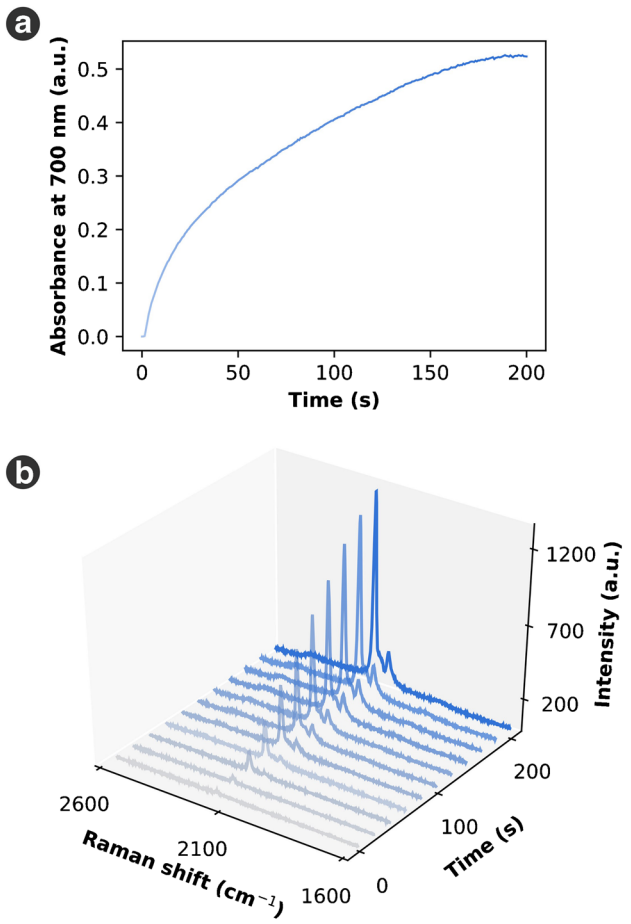

Fig. 4. In situ film growth measurements using lab-made 3D-printed accessories for spectroelectrochemistry: (**a**) Scatter plot of the in situ absorption monitoring at 700 nm using UV-VIS Spectroelectrochemical cell. (**b**) Scattering spectra as a function of time using Raman spectroelectrochemical cell, during the electrodeposition of Prussian Blue film in the lab-made platinum working electrode surface in 0.1 mol L^{-1} KCl solution

0.1 mol L^{-1} KCl solution, after washing and purging the cells with ultrapure water and the new medium. A voltammogram between −0.3 and 1.1 V was taken for electrochemical evidence of film formation and maintenance (see Supporting Information Section S.5, Fig. S.19). The film was converted to the other forms by applying a potential of −0.3 V and 1.1 V for conversion to PW and BG forms, respectively. The conversion potential was maintained during the spectra acquisition process, whose responses were taken as referring to the pure forms of those states [20]. The two distinct pairs of redox peaks correspond to the oxidation of PW to PB (close to 0.3 V, Eq. 3) and the oxidation of PB to BG (at approximately 1.0 V, Eq. 4). The redox behavior of the PB film can be expressed according to the following equations:

$$K_4Fe_4^{(II)}\left[Fe^{(II)}(CN)_6\right]_3 \rightleftarrows Fe_4^{(III)}\left[Fe^{(II)}(CN)_6\right]_3 + 4K^+ + 4e^- \quad (3)$$

$$Fe_4^{(III)}\left[Fe^{(II)}(CN)_6\right]_3 - 3e^- + 3Cl^- \rightleftarrows Fe_4^{(III)}\left[Fe^{(III)}(CN)_6Cl\right]_3 \quad (4)$$

Figure 5 shows the simultaneous control of the applied potential and the spectroscopic information using the UV-VIS and Raman SECs.

One can observe when analyzing Fig. 5a.1 that the absorption band at 700 nm was assigned to the intervalence charge transfer from the Fe(II)-C to Fe(III)-N (reason of the blue color). This signal was attenuated with the reduction of the Fe (III) sites when the film was converted to the PW form by application of −0.1 V *vs.* Ag/AgCl (3M KCl) as can be observed in Fig. 5a.2. In highly anodic potentials, the PB was converted on BG, whose absorption band (near than 400 nm) can be associated to crystal field transitions (Fig. 5a.3) [23–25]. In the Raman spectroscopy investigations (Fig. 5b.1), PB forms can be characterized through the presence of (CN) bands between 2000 and 2200 cm^{-1}. The frequency of the CN^- vibrational stretching mode depends upon the oxidation state of the metal cation coordinated to the cyanide anions, and also their electronegativity. The cyanide group tends to act as a σ-donor, so as the metal-carbon bond increases, by increasing the metal electron density or metal charge, the electron density from the antibonding orbital is reduced in the C≡N bond, which strengthens that bond and increases its vibrational frequency [26]. As a mixed-valence compound, PB showed two sharp bands in that interval that can be assigned to the A_{1g} and E_g (CN) modes of the CN^- anion: the lower frequency band at 2092 cm^{-1} can be linked to a (CN) mode associated with Fe(II) cation, whereas the higher frequency band at approximately 2156 cm^{-1} can be assigned to a ν(CN) mode associated with Fe(III) cation. At cathodic potentials (Fig 5b.2), a completely different pattern was observed, with the appearance of (CN) scattering at 2136, 2103, and 2048 cm^{-1}, due to the conversion to PW form. On the other hand, at anodic potentials, the Raman spectrum (Fig. 5b.3) exhibits a band at 2155 cm^{-1} and a broad shoulder at lower frequencies, as a consequence of the higher oxidation state of most of the Fe cations caused by the electrochemical film conversion to the BG form [27, 28]. Table 1 summarizes the main features of the 3D printing lab-made accessories for spectroelectrochemical measurements as well as useful corresponding references where more detailed information can be obtained if necessary.

Conclusions

The results obtained in this work demonstrated the capacity of 3D FDM printing as a technology to produce rapid accessories prototyping for spectroscopy and spectroelectrochemistry. The cells were properly designed using PETg-based

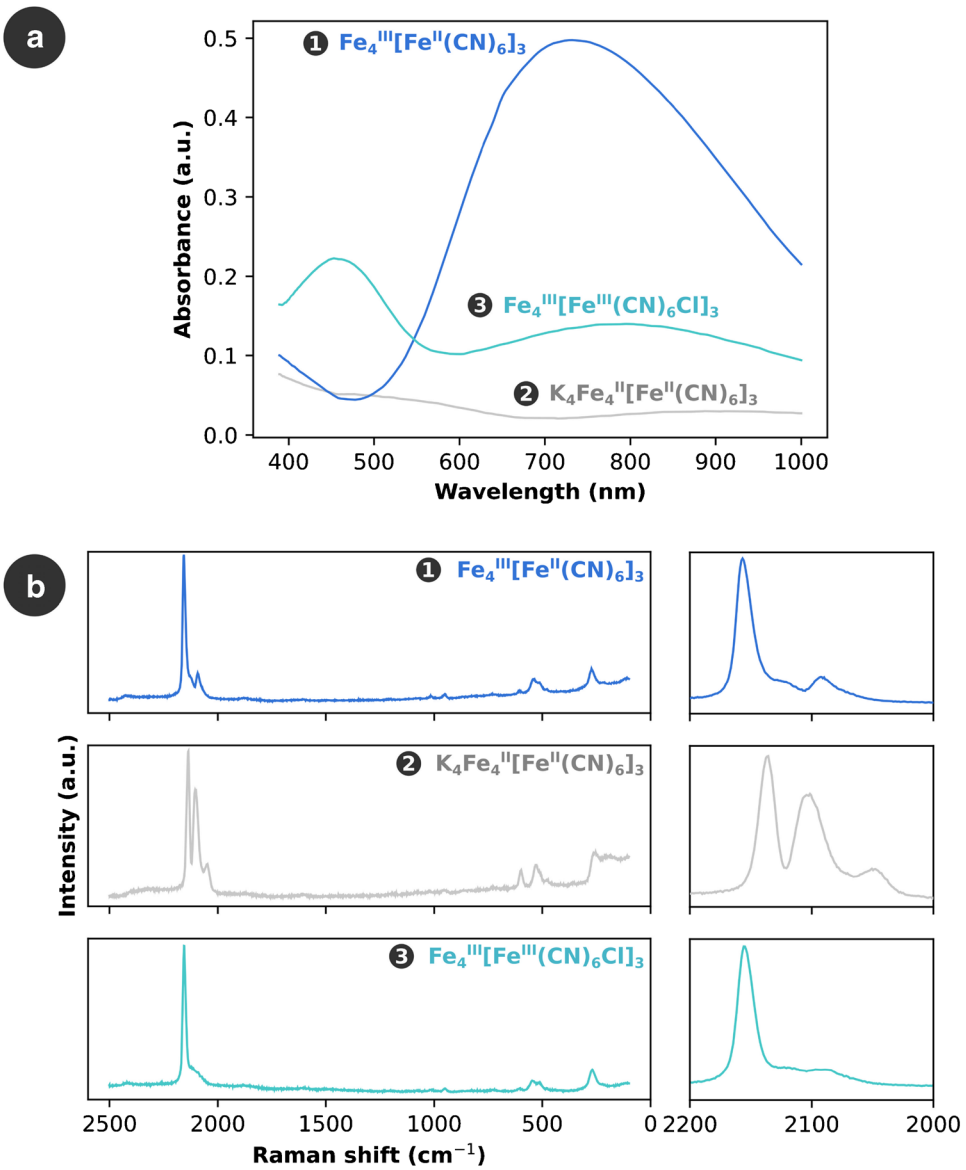

Fig. 5. In situ electrochemical conversion of Prussian Blue film in a lab-made platinum working electrode in 0.1 mol L^{-1} KCl solution using lab-made 3D-printed accessories for spectroelectrochemistry (**a**) UV-VIS reflection-absorption spectra. (**b**) Raman scattering spectra of the three different redox states of the film: (1) Prussian Blue by applying 0.5 V, (2) Prussian White by applying −0.3 V, and (3) Berlin Green by applying 1.1 V vs. Ag/AgCl/KCl(sat)

filament, being it a cheap, inert, durable, versatile, and sustainable material. Thus, this powerful technique was used to produce robust alternatives accessories for ex situ specular reflectance spectroscopy and spectroelectrochemical cells suitable for in situ Raman and UV-VIS spectroscopy measurements.

Furthermore, accessories and cells were tested using Allura Red AC dye and PB-electrodeposited films as reference materials/processes. It was possible to obtain spectroscopic measurements of the films and observe in situ growth and structural changes during the redox processes suffered by PB. The specular reflectance accessory allows adaptation to receive electrodes as a sample, and the spectroelectrochemical cells were designed to receive standard ⌀6 mm electrodes although the accessories can be easily adapted to any other needs—the projects are ideas that can be improved by linking up the demands of industry and research institutions. Finally, similar studies can be carried out in analogous processes as kinetics and reaction mechanisms estimations, the study of shorter-lived species, localized interfacial investigations, and surface modifications analysis considering the innovative designs and new analytical strategies capacity of these new tools. Reflectance measurements mediated by accessories can be appropriately performed on different materials, and are applicable to the characterization of polymers, ceramics, dyes, pigments, semiconductors, etc.

Table 1 Overview of lab-made accessories for spectroelectrochemical measurements

System	Analytical application	Manufacturing feature	Advantages	Drawbacks	Ref.
Thin layer SEC	In situ IRRAS spectroelectrochemical measurements	Adaptation from a pre-existing reflection module	Simple design Variable temperature feature	Very specific working electrode Not easily reproducible	[4]
Thin layer SEC	In situ UV-VIS-IRRAS measurements	PEEK-machined parts and quartz or CaF_2 window for UV-Vis and IR region, respectively	Simple design Versatile	Specific electrodes Its use requires extra adaptations or accessories in some coupled techniques	[5]
Thin layer SEC	IR, UV-VIS, Raman, XAS, and XRD In situ experiments	PEEK-machined parts and CaF_2 or quartz windows for IR and UV-Vis-Raman experiments, respectively	Simple design Highly versatile Allows to perform experiments in flux Compatible with common commercial electrodes	Its use requires extra adaptations or accessories in most coupled techniques	[6]
Thin layer SEC	Ultrafast 2D-IR In situ measurements	PEEK-machined parts and CaF_2 window	Variable temperature feature Very small sample volume (a few microliters)	Not easily reproducible	[7]
Thin layer SEC	In situ Raman spectroelectrochemical experiments	PEEK-machined parts with a quartz window	Simple design Easy (dis)assemble Small sample volume	Not easily reproducible	[8]
Thin layer SEC	In situ Raman spectroelectrochemical experiments	3D printed (ABS filament)	Minimum manipulation of working electrode Low-cost Low-time production Easily reproducible	Very specific working electrode Absence of window may compromise microscope objectives	[10]
Thin layer SEC	In situ Raman spectroelectrochemical experiments	3D printed (ABS filament)	Simple design Easy (dis)assemble Low-cost Low-time production Easily reproducible Very specific working electrode	Absence of window may compromise microscope objectives Design reduces the ability to perform Raman imaging measurements	[11]
Thin layer SEC	UV-VIS In situ spectroelectrochemical experiments	3D printed (Fullcure 720 acrylic polymer)	Simple design Easy assemble in a standard cuvette Low-cost Very small sample volume	Very specific working electrode Just applicable for transmission measurements Not easily reproducible	[12]
Multi-purpose electrochemical device for x-ray spectroscopy	In operando x-ray absorption spectroscopy	3D printed (photopolymer resin)	Simple design Inexpensive Low-time production Small sample volume	Very specific electrodes required	[13]

Table 1 (continued)

System	Analytical application	Manufacturing feature	Advantages	Drawbacks	Ref.
Transmission UV-Vis SEC	UV-VIS In situ spectroelectrochemical experiments	3D printed (PLA filament)	Easy assemble in a standard cuvette-holder Low-cost Low-time production Versatile Easily reproducible	Just applicable for transmission measurements	[14]
General-purpose module for specular spectroscopy	UV-VIS-NIR and FTIR reflectance-based measurements	3D printed (PETg filament)	Simple design Low-cost Low-time production Versatile Easily reproducible	Just applicable for ex situ measurements	This work
Thin layer SEC	UV-VIS-NIR in situ spectroelectrochemical experiments	3D printed (PETg filament) and a quartz window	Simple design Low-cost Low-time production Compatible with common commercial electrodes Easily reproducible	Lab-made mirrors may attenuate the reflectivity signal, especially from UV region	This work
Thin layer SEC	In situ Raman spectroelectrochemical experiments	3D printed (PETg filament) and a quartz window	Easy (dis)assemble Low-cost Low-time production Compatible with common commercial electrodes Allows to perform experiments in flux Easily reproducible	Designed for ⌀6 mm electrodes	This work

Supplementary Information The online version contains supplementary material available at https://doi.org/10.1007/s00604-021-05041-3.

Acknowledgments The authors acknowledge financial support from FINEP (Financiadora de Estudos e Projetos) and are also very grateful to Central Analítica of Chemistry Institute—UFRN for all infrastructure and equipment.

Declarations

Conflict of interest The authors declare they have no competing interests.

References

1. Bard AJ, Faulkner LR (1980) Electrochemical Methods. John Wiley & Sons, New York
2. Kaim W, Fiedler J (2009) Spectroelectrochemistry: the best of two worlds. Chem Soc Rev 38:3373–3382. https://doi.org/10.1039/B504286K
3. Lozeman JJA et al (2020) Spectroelectrochemistry, the future of visualizing electrode processes by hyphenating electrochemistry with spectroscopic techniques. Analyst 145:2482–2509. https://doi.org/10.1039/c9an02105a
4. Zaravine IS, Kubiak CP (2001) A versatile variable temperature thin layer reflectance spectroelectrochemical cell. J Electroanal Chem 491:106–109. https://doi.org/10.1016/S0022-0728(00)00394-6
5. Bernad S, Mantele W (2006) An innovative spectroelectrochemical reXection cell for rapid protein electrochemistry and ultraviolet/visible/infrared spectroscopy. Anal Biochem 351:214–218. https://doi.org/10.1016/j.ab.2005.12.024
6. Bott-Neto JL et al (2020) Versatile Spectroelectrochemical Cell for In Situ Experiments: Development, Application, and Electrochemical Behaviour. ChemElectroChem 7:1–9. https://doi.org/10.1002/celc.202000910
7. Khoury YE et al (2015) A spectroelectrochemical cell for ultrafast two-dimensional infrared spectroscopy. Rev. Sci. Instrum. 86:083102. https://doi.org/10.1063/1.4927533
8. Timm RA et al (2016) Versatile and low cost spectroelectrochemical cell for in situ study of electrode surfaces. Electrochim Acta 232:150–155. https://doi.org/10.1016/j.electacta.2017.02.132
9. Vaněčková E et al (2020) UV/VIS spectroelectrochemistry with 3D printed electrodes. J Electroanal Chem 857:113760. https://doi.org/10.1016/j.jelechem.2019.113760
10. da Silveira GD et al (2021) Ready-to-use 3D-printed electrochemical cell for in situ voltammetry of immobilized microparticles and Raman spectroscopy. Anal Chim Acta 1141:57–62. https://doi.org/10.1016/j.aca.2020.10.023
11. dos Santos MF et al (2019) 3D-Printed Low-Cost Spectroelectrochemical Cell for In Situ Raman Measurements. Anal Chem 91:10386–10389. https://doi.org/10.1021/acs.analchem.9b01518
12. Brisendine JM et al (2013) A three-dimensional printed cell for rapid, low-volume spectroelectrochemistry. Anal Biochem 439:1–3. https://doi.org/10.1016/j.ab.2013.03.036
13. Achilli E et al (2016) 3D-printed photo-spectroelectrochemical devices for in situ and in operando X-ray absorption spectroscopy investigation. J Synchrotron Rad 23:622–628. https://doi.org/10.1107/S1600577515024480
14. Whitehead HD et al (2017) 3D Printed UV−Visible Cuvette Adapter for Low-Cost and Versatile Spectroscopic Experiments. ACS Omega 2:6118–6122. https://doi.org/10.1021/acsomega.7b01310
15. Ambrosi A, Shi RRS, Webster RD (2020) 3D-printing for electrolytic processes and electrochemical flow systems. J Mater Chem A 8:21902–21929. https://doi.org/10.1039/d0ta07939a
16. Ambrosi A, Bonanni A (2021) How 3D printing can boost advances in analytical and bioanalytical chemistry. Microchim Acta 188:265–282. https://doi.org/10.1007/s00604-021-04901-2
17. Ambrosi A, Pumera M (2016) 3D-printing technologies for electrochemical applications. Chem Soc Rev 45:2740–2755. https://doi.org/10.1039/C5CS00714C
18. Cardoso RM et al (2020) Additive-manufactured (3D-printed) electrochemical sensors: A critical review. Anal Chim Acta 1118:73–91. https://doi.org/10.1016/j.aca.2020.03.028
19. Silva AL et al (2021) A 3D Printer Guide for the Development and Application of Electrochemical Cells and Devices. Front Chem 9:684256. https://doi.org/10.3389/fchem.2021.684256
20. Wang L, Pumera M (2021) Recent advances of 3D printing in analytical chemistry: Focus on microfluidic, separation, and extraction devices. TrAC Trend Anal Chem 135:116151. https://doi.org/10.1016/j.trac.2020.116151
21. Bevziuk K et al (2017) Spectrophotometric and theoretical studies of the protonation of Allura Red AC and Ponceau 4R. J Mol Struct 1144:216–224. https://doi.org/10.1016/j.molstruc.2017.05.001
22. Ávila-MArtínez AK et al (2020) Allura Red dye sorption onto electrospun zirconia nanofibers. Environ Technol Inno 18:100760. https://doi.org/10.1016/j.eti.2020.100760
23. Garcia-Jareno JJ, Navarro-Laboulais J, Vicente F (1998) Electrochemical Behavior of Electrodeposited Prussian Blue Films on ITO Electrode: An Attractive Laboratory Experience. J Chem Educ 75:881. https://doi.org/10.1021/ed075p881
24. Hegner FS, Galán-Mascarós JR, López N (2016) A Database of the Structural and Electronic Properties of Prussian Blue, Prussian White, and Berlin Green Compounds through Density Functional Theory. Inorg Chem 55:12851–12862. https://doi.org/10.1021/acs.inorgchem.6b02200
25. Cheng K, Chen F, Kai J (2007) Electrochromic property of nano-composite Prussian Blue based thin film. Electrochim Acta 52:3330–3335. https://doi.org/10.1016/j.electacta.2006.10.012
26. Moretti G, Gervais C (2018) Raman spectroscopy of the photosensitive pigment Prussian blue. J Raman Spectrosc 49:1198–1204. https://doi.org/10.1002/jrs.5366
27. Samain L et al (2013) Redox reactions in Prussian blue containing paint layers as a result of light exposure. J Anal At Spectrom 28:524–535. https://doi.org/10.1039/C3JA30359D
28. Nossol E, Zarbin AJG (2012) Transparent films from carbon nanotubes/Prussian blue nanocomposites: preparation, characterization, and application as electrochemical sensors. J Mat Chem 22:1824–1833. https://doi.org/10.1039/C1JM14225A